



An X-shaped solution-processible oligomer having an anthracene unit as a core: A new organic light-emitting material with high thermostability and efficiency

Jing Sun^a, Hongliang Zhong^a, Erjian Xu^a, Danli Zeng^a, Jianhua Zhang^b, Hongguang Xu^c, Wenqing Zhu^b, Qiang Fang^{a,*}

^a Key Laboratory of Organofluorine Chemistry and Laboratory for Polymer Materials Shanghai Institute of Organic Chemistry, Chinese Academy of Sciences, 345 Lingling Road, Shanghai 200032, PR China

^b Key Laboratory of Advanced Display and System Applications, Shanghai University, Ministry of Education, 149 Yanchang Road, Shanghai 200072, PR China

^c R&D Center for Flat Panel Display Technology, SVA Company, Shanghai 200081, PR China

ARTICLE INFO

Article history:

Received 13 July 2009

Received in revised form 17 September 2009

Accepted 30 September 2009

Available online 20 October 2009

Keywords:

Organic light-emitting diodes

π -Conjugated oligomers

Anthracene derivatives

Optical properties

Electrochemical properties

ABSTRACT

A new X-shaped solution-processible oligomer with a glass transition temperature of higher than 200 °C based on an anthracene derivative was prepared, and it showed good hole-transporting ability in organic light-emitting diodes (OLED). Such oligomer was also employed as the emitting layer to give the devices showing blue emission.

© 2009 Elsevier B.V. All rights reserved.

1. Introduction

In the recent years, there has been an increasing interest in the synthesis and characterization of the π -conjugated molecules with topologically special structure such as cruciform or X-shaped [1–12]. Those molecules show highly electrochemical and photoluminescent activities, and easily form amorphous glass in the solid state. Moreover, some of them display sensitivity to proton and metals [2,3]. Such interesting properties of the molecules are desired for the application in optoelectronic field as the

materials in non-linear optical device [4,5], light-emitting diodes [7,11], organic field-effect transistors [12] and chemical sensors [2,3].

Compared with the linear conjugated molecules, the conjugated cruciform compounds show spatially separated energy levels of HOMO and LUMO, and each branch of the molecules possess independent properties, which are suitable for the applications of chemical sensors [2]. It is more important the π -aggregation is depressed in the conjugated cruciform molecules due to the special 3D structure of the molecules [13], and such properties probably are useful for fabrication of the optoelectronic devices with excellent properties. Undoubtedly, investigation on the relationship between the chemical structure of the cruciform compounds and properties of the molecules is very necessary.

* Corresponding author. Tel./fax: +86 21 5492 5337.

E-mail address: qiangfang@mail.sioc.ac.cn (Q. Fang).

It is noted that there are few building models for the cruciform compounds. E.g., the reported cruciform molecules are mainly formed by the models that each branch of the molecules is extended from a benzene (or a thiophene) ring [14,15]. Thus, exploring and developing new building models of the π -conjugated molecules with cruciform structure are desired.

To build a new structure of the cruciform compounds, a better choice is employing anthracene as a starting unit because an anthracene unit possesses four active positions, e.g., 2,6- and 9,10-positions, in which the covalent bonds are easily formed. When an anthracene unit contains π -conjugated substituted groups both at 2,6- and 9,10-positions, those molecules are topologically cross-shaped (or X-shaped). On the other hand, anthracene-based derivatives have been widely used as organic optoelectronic materials owing to their high fluorescence quantum yields [16], implying that studying the derivatives with new structure is helpful to find new kind of the anthracene-based materials. Hence, we designed and synthesized a new anthracene-based oligomer **8**, whose structure is shown in Scheme 1. Such oligomer shows good hole-transporting ability in organic light-emitting diodes. Moreover, employing the oligomer as the emitting layer gives the devices showing blue emission. Herein, we report the details.

2. Experimental

2.1. Materials

2,7-Dibromo-9,9-diethyl-fluorene (**1**) [17a], 2,6-dibromoanthraquinone (**4**) [17b], pinacol(4-(*N,N*-diphenylamino)-phenyl)boronate (**6**) [17c] were prepared as previously reported. $[\text{Bu}_4\text{N}]\text{ClO}_4$ (Bu = butyl) was an industrial product and purified by recrystallized three times from a mixture of ethyl acetate and cyclohexane and dried over P_2O_5 under vacuum at room temperature for three days. All solvents were dehydrated and distilled under an inert atmosphere before use.

2.2. Instrumentation

Elemental analysis was taken with a Carlo Erba 1106 elemental analyzer. ^1H NMR spectra were carried out on a Bruker DRX 300 spectrometer and ^{13}C NMR spectra were carried out on a Bruker DRX 400 spectrometer. UV–Vis absorption and photoluminescence spectra were measured with a Hitachi U-2910 spectrophotometer and a Hitachi F-4500 fluorescence spectrophotometer, respectively. Cyclic voltammetry (CV) for the cast films were measured in an acetonitrile solution of $[\text{Bu}_4\text{N}]\text{ClO}_4$ (0.10 M, Bu = butyl) at a scan rate of 100 mV/s under argon using (0.10 M AgNO_3)/Ag and platinum wire as reference and counter electrodes, respectively. A CHI 600B analyzer was used for the measurements. DSC was determined with TA Instrument DSC Q200 at a heating and cooling rate of $10^\circ\text{C min}^{-1}$ under nitrogen flow.

2.3. LED device fabrication

On a cleaning ITO glass, a layer PEDOT-PSS (50 nm, Bayer AG) was applied. A layer of **11** (10 mg/mL in CHCl_3 for the application of hole-transporting layer, 20 mg/mL in CHCl_3 for the application of light-emitting layer) was then spin-coated on the substrate. After dried 2 h in a glove box at 60°C , Alq_3 (30 nm), LiF, Ca (120 nm) and Al (100 nm) were deposited on the compound film by thermal evaporation, respectively, under a vacuum of 10^{-4} Pa. The measurements of the properties of the devices were operated at room temperature in air. The EL spectra were recorded on a photometer PR 705.

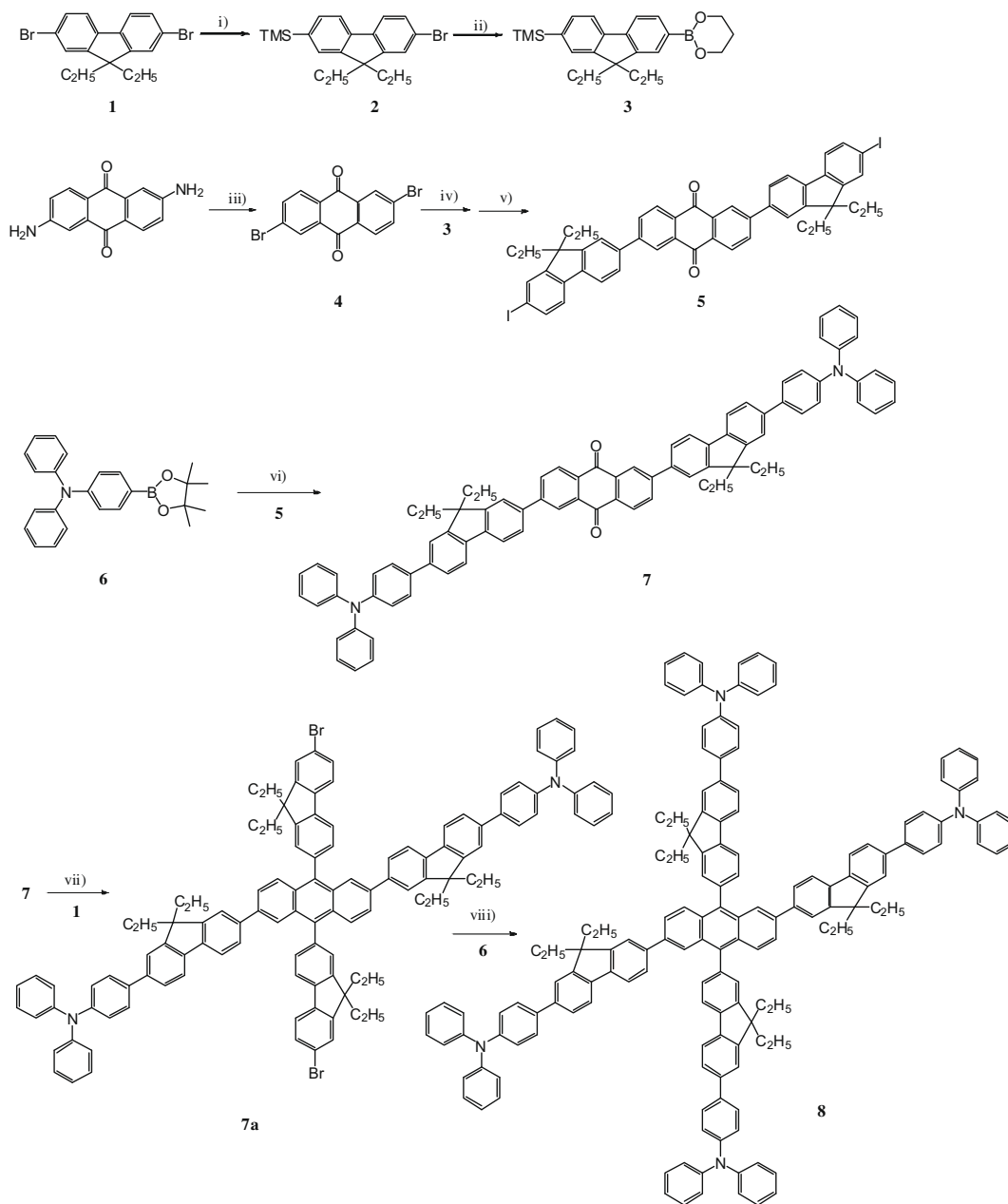
2.4. Synthesis of the compounds

2.4.1. Synthesis of (2-bromo-9,9-diethyl-9H-fluorene-7-yl)trimethylsilane (**2**)

Under an argon atmosphere, a solution of *n*-BuLi in hexane (1.6 M, 11.8 mL, 18.8 mmol) was added slowly at -78°C to a solution of **1** in anhydrous THF. The mixture was stirred for 1 h at -78°C before adding chlorotrimethylsilane (6.0 g, 55.3 mmol). The reactants were warmed to room temperature and stirred for 3 h, poured into water of 200 mL, and extracted with hexane. The organic layer was washed with water and dried over Na_2SO_4 . **2** was obtained as a colorless oil by column chromatography on silica gel with hexane as the eluent. 6.80 g, yield of 99%. ^1H NMR (300 MHz, CDCl_3 , δ in ppm): 7.68 (d, 1H), 7.69 (d, 1H), 7.52 (d, 1H), 7.46–7.49 (m, 3H), 2.04 (m, 4H), 0.33–0.38 (m, 15H).

2.4.2. Synthesis of (7-(1,3,2-dioxaborinan-2-yl)-9,9-diethyl-9H-fluorene-2-yl)trimethylsilane (**3**)

A solution of *n*-BuLi in hexane (1.6 M, 12.5 mL, 20.0 mmol) was added slowly to a solution of **2** (6.79 g, 18.2 mmol) in anhydrous THF (80 mL) at -78°C . The mixture was stirred for 1 h at -78°C before triisopropyl boronate (10.3 g, 54.6 mmol) was added. The reactants were warmed to room temperature, stirred for 24 h, poured into a large amount of water (200 mL), and extracted with ethyl acetate. The organic layer was washed with brine and dried over Na_2SO_4 . After removal of the solvent under reduced pressure, the residue was obtained as the boric acid (6.05 g, yield of 98.4%) as white solid. To a solution of the boric acid (6.05 g, 17.9 mmol) in toluene (150 mL), 1,3-propanediol (4.15 g, 54.6 mmol) was added, and the mixture was stirred at 110°C for 10 h. After being cooled to room temperature, the solution was washed with water, dried over Na_2SO_4 , and evaporated to remove the solvent. The obtained crude product was purified by column chromatography using a mixture solvent of hexane and ethyl acetate (8:1, v/v) as the eluent to afford a white solid **3** (6.30 g, yield of 93.1%). ^1H NMR (300 MHz, CDCl_3 , δ in ppm): 7.69–7.78 (m, 4H), 7.47 (m, 2H), 4.21 (t, 4H), 2.06 (m, 6H), 0.27–0.32 (m, 15H). ^{13}C NMR (100 MHz, CDCl_3 , δ in ppm): 149.56, 149.13, 143.90, 142.11, 139.38, 132.46, 131.76, 127.91, 127.54, 119.22, 118.96, 62.02, 55.89, 32.60, 27.46, 8.59. FT-IR (KBr pellets, cm^{-1}): 2960, 2852, 1608, 1482,



Scheme 1. Synthetic procedure of the oligomer **8**. Reagents and conditions: (i) (1) *n*-BuLi, THF, $-78\text{ }^{\circ}\text{C}$, (2) TMSCl, $-78\text{ }^{\circ}\text{C}$ to room temperature; (ii) (1) *n*-BuLi, THF, $-78\text{ }^{\circ}\text{C}$, (2) *(i*-PrO)₃B, $-78\text{ }^{\circ}\text{C}$ to room temperature; (3) 1,3-propanediol, toluene, $110\text{ }^{\circ}\text{C}$; (iii) *t*-BuONO, CuBr₂, CH₃CN, $65\text{ }^{\circ}\text{C}$; (iv) Pd(PPh₃)₄, aq. K₂CO₃, toluene, $80\text{ }^{\circ}\text{C}$; (v) ICl, CHCl₃, $0\text{ }^{\circ}\text{C}$ to room temperature; (vi) Pd(PPh₃)₄, aq. K₂CO₃, toluene, $80\text{ }^{\circ}\text{C}$; (vii) 1) *n*-BuLi, THF, (2) KI, NaH₂PO₂·H₂O, AcOH, $120\text{ }^{\circ}\text{C}$; (viii) Pd(PPh₃)₄, K₂CO₃, THF, $80\text{ }^{\circ}\text{C}$.

1426, 1313, 1277, 1250, 1230, 1156, 1266, 857, 841, 820, 754, 684. MS (EI): 378 (*M*⁺).

2.4.3. Synthesis of 2,6-dibromoanthraquinone (**4**)

2,6-Diaminoanthraquinone (2.9 g, 12 mmol) was added to a solution of *t*-BuONO (3.62 mL, 2.8 g, 27 mmol) and CuBr₂ (6.0 g, 27 mmol) in CH₃CN (50 mL) at $65\text{ }^{\circ}\text{C}$. The mixture was stirred for 3 h and then slowly poured into 20% aqueous HCl solution (200 mL). The precipice was filtered,

washed with water, CH₃CN, and benzene. Finally, the more pure product was obtained by washing with benzene. (3.75 g, yield of 84%).

2.4.4. Synthesis of 2,6-bis(9,9-diethyl-7-iodo-9H-fluoren-2-yl) anthraquinone (**5**)

Under an argon atmosphere, a mixture of **4** (1.85 g, 5.07 mmol), **3** (4.31 g, 11.4 mmol), Pd(PPh₃)₄ (0.29 g, 0.25 mmol) and K₂CO₃ (3.22 g, 23.3 mmol) in THF

(80 mL) and distilled water (40 mL) was stirred for 48 h at 80 °C. After being cooled to room temperature, the mixture was extracted with CHCl₃. The organic layer was washed with water and dried over with anhydrous Na₂SO₄. After removal of the solvents, the residue was recrystallized with a mixture solvent of toluene and ethanol to yield a yellow solid, which was dissolved in anhydrous CHCl₃ (3.02 g in 60 mL), and to the obtained solution was added a mixture of ICl in methylene chloride solution (1.0 M, 8.4 mL, 8.4 mmol) under an argon atmosphere at 0 °C. After warmed to room temperature, the reactants were stirred for 4 h, then poured into aqueous NaHSO₃ (5% w/w, 200 mL). The mixture was extracted with CHCl₃ and the organic layer was washed with water before being dried over with Na₂SO₄. After evaporated to remove the solvent, the residue was purified by recrystallization with toluene to give **5** as a crude product with a yield of 69%. ¹H NMR (300 MHz, CDCl₃, δ in ppm): 8.64 (s, 2H), 8.45 (d, 2H), 8.12 (d, 2H), 7.83 (d, 2H), 7.69–7.77 (m, 8H), 7.53 (d, 2H), 2.11 (m, 8H), 0.37 (t, 12H). ¹³C NMR (100 MHz, CDCl₃, δ in ppm): 183.11, 152.75, 150.46, 147.25, 141.95, 140.36, 138.14, 134.12, 132.36, 132.28, 132.16, 128.18, 126.61, 125.51, 121.73, 121.62, 120.45, 93.26, 56.70, 32.73, 8.56. FT-IR (KBr pellets, cm⁻¹): 2958, 1672, 1592, 1453, 1399, 1313, 969, 816, 746, 479. MS (MALDF-TOF): 900.3 (M⁺).

2.4.5. Synthesis of 2,6-bis(7-(4-(diphenylamino)phenyl)-9,9-diethyl-9H-fluoren-2-yl)-anthraquinone (**7**)

Under an argon atmosphere, a mixture of **5** (1.88 g, 2.08 mmol), **6** (1.70 g, 4.58 mmol), Pd(PPh₃)₄ (0.12 g, 0.10 mmol) and K₂CO₃ (1.32 g, 9.57 mmol) in THF (50 mL) and distilled water (25 mL) was stirred for 48 h at 80 °C. After being cooled to room temperature, the mixture was extracted with CHCl₃. The organic layer was washed with water and dried over anhydrous Na₂SO₄. After removal of the solvents, the residue was purified by column chromatography on silica gel using a mixture solvent of petroleum ether and CH₂Cl₂ (1:1, v/v) as the eluent to obtain **7** as an orange powder (1.98 g, yield of 83.8%). ¹H NMR (300 MHz, CDCl₃, δ in ppm): 8.67 (d, 2H), 7.46 (d, 2H), 8.14 (d, 2H), 7.23–7.88 (m, 8H), 7.27–7.32 (m, 8H), 7.17 (m, 12H), 7.05 (m, 4H), 2.16 (m, 8H), 0.42 (t, 12H). ¹³C NMR (100 MHz, CDCl₃, δ in ppm): 138.41, 151.50, 151.31, 147.91, 147.68, 147.45, 142.55, 140.41, 139.79, 137.82, 135.62, 134.37, 132.51, 132.29, 129.53, 128.39, 128.06, 126.74, 125.89, 125.67, 124.62, 124.27, 123.19, 121.68, 121.31, 120.60, 120.50, 56.74, 33.14, 8.91. FT-IR (KBr pellets, cm⁻¹): 3032, 2962, 2874, 1673, 1591, 1514, 1492, 1464, 1377, 1310, 1281, 817, 747, 695, 497. MS (MALDF-TOF): 1136.0 (M⁺). Elemental analysis: Calcd for C₈₄H₆₈N₂O₂: C, 88.86; H, 5.86; N, 2.47. Found: C, 88.77; H, 6.00; N, 2.13.

2.4.6. Synthesis of 2,6,9,10-tetra(7-(4-(diphenylamino)phenyl)-9,9-diethyl-9H-fluoren-2-yl)-anthracene (**8**)

A solution of *n*-BuLi (1.6 M, 1.38 mL, 2.21 mmol) in hexane was added slowly to a solution of **1** (839 mg, 2.21 mmol) in anhydrous THF (30 mL) at –78 °C, and the mixture was stirred for 1 h at the same temperature. Then a solution of **7** (627 mg, 0.55 mmol) in anhydrous THF was

added to the mixture. The reactants were allowed to slowly warm to room temperature, stirred for 24 h and poured to water of 200 mL. The mixture was extracted with ethyl acetate, and the obtained organic layer was washed with brine and dried over Na₂SO₄. Column chromatography on silica gel with hexane:CHCl₃:ethyl acetate (30:10:4) as the eluent afford an intermediate (901 mg, yield of 93.8%) as an orange glass. ¹H NMR (300 MHz, CDCl₃, δ in ppm): 7.86 (s, 2H), 7.41–7.72 (m, 32H), 7.25–7.30 (m, 8H), 7.16 (m, 12H), 7.04 (m, 4H), 3.36 (s, 2H), 1.96–2.11 (m, 16H), 0.27–0.41 (m, 24H). ¹³C NMR (100 MHz, CDCl₃, δ in ppm): 152.76, 151.03, 149.60, 147.92, 147.32, 145.96, 142.06, 141.77, 141.10, 140.44, 140.05, 139.88, 139.81, 139.19, 135.75, 130.33, 129.51, 129.33, 128.03, 127.30, 126.50, 126.21, 125.83, 124.57, 124.31, 123.13, 121.75, 121.42, 121.35, 121.28, 121.21, 120.35, 120.08, 119.55, 76.94, 56.85, 56.44, 32.97, 8.88, 8.65. FT-IR (KBr pellets, cm⁻¹): 3543, 3033, 2963, 2920, 2875, 2852, 1592, 1514, 1493, 1464, 1377, 1313, 1279, 1006, 908, 815, 753, 734, 697. MS (MALDF-TOF): 1738.3 (M⁺).

Under an argon atmosphere, the above mentioned intermediate (901 mg, 0.52 mmol), was added to a mixture of potassium iodide (861 mg, 5.2 mmol) and sodium hypophosphite hydrate (1.10 g, 10.4 mmol) in acetic acid (50 mL), and the mixture was stirred for 19 h at 120 °C. After being cooling to room temperature, the mixture was filtered and washed with water. The residue was purified by column chromatography on silica gel using a mixture of petroleum ether and CHCl₃ (2:1, v/v) as the eluent to give **7a** as a green–yellow powder, 658 mg, yield of 74.5%. ¹H NMR (300 MHz, CDCl₃, δ in ppm): 8.06 (s, 2H), 7.98 (d, 2H), 7.90 (d, 2H), 7.64–7.79 (m, 8H), 7.50–7.59 (m, 20H), 7.25–7.31 (m, 8H), 7.13–7.17 (m, 12H), 7.04 (m, 4H), 1.97–2.14 (m, 16H), 0.53 (m, 12H), 0.28–0.38 (m, 12H). ¹³C NMR (100 MHz, CDCl₃, δ in ppm): 152.42, 150.87, 150.81, 149.78, 147.67, 147.05, 139.83, 139.54, 138.53, 137.57, 135.51, 130.40, 130.22, 129.60, 129.24, 127.74, 127.57, 126.33, 125.57, 125.45, 124.31, 124.05, 122.86, 121.48, 121.37, 121.17, 120.96, 119.96, 119.89, 56.72, 56.14, 32.82, 32.69, 8.70, 8.58. FT-IR (KBr pellets, cm⁻¹): 2962, 2918, 2974, 2851, 1592, 1541, 1493, 1455, 1377, 1313, 1278, 883, 812,752, 754, 696. MS (MALDF-TOF): 1702.8 ((M-1)⁺). Elemental analysis: Calcd for C₁₁₈H₉₈Br₂N₂: C, 83.18; H, 5.80; N, 1.64; Br, 9.38. Found: C, 82.93; H, 6.10; N, 1.61; Br, 9.32.

The obtained green–yellow powder (200 mg, 0.12 mmol), mentioned above was added to a mixture of **6** (96 mg, 0.26 mmol), Pd(PPh₃)₄ (14 mg, 0.012 mmol) and K₂CO₃ (250 mg, 1.81 mmol) in THF (40 mL) containing distilled water (15 mL). The reactants were stirred for 48 h at 80 °C. After being cooled to room temperature, the mixture was extracted with CHCl₃. The organic layer was washed with water and dried over with anhydrous Na₂SO₄. After removal of the solvent, the residue was purified by column chromatography on silica gel using a mixture solvent of petroleum ether and CH₂Cl₂ (3:2, v/v) as the eluent to give **8** as a yellow–green powder, 190 mg, yield of 79.5%. ¹H NMR (300 MHz, CDCl₃, δ in ppm): 8.12 (s, 2H), 8.02 (d, 2H), 7.94 (m, 4H), 7.78 (d, 2H), 7.61–7.71 (m, 14H), 7.49–7.58 (m, 14H), 7.23–7.33 (m, 18H), 7.12–7.22 (m, 22H), 7.05 (m, 8H), 2.17 (m, 8H), 1.99

(m, 8H), 0.54–0.60 (m, 12H), 0.28–0.38 (m, 12H). ^{13}C NMR (100 MHz, CDCl_3 , δ in ppm): 150.91, 150.82, 150.33, 147.72, 147.68, 147.13, 147.03, 140.87, 140.62, 140.36, 139.92, 139.75, 139.65, 139.53, 137.81, 137.68, 135.62, 135.84, 130.51, 130.25, 129.71, 129.29, 127.84, 127.75, 126.18, 126.05, 125.74, 125.56, 125.36, 124.53, 124.34, 124.17, 124.08, 122.90, 122.86, 121.51, 121.05, 120.97, 120.10, 119.52, 119.91, 119.77, 56.48, 56.16, 33.12, 33.01, 8.84, 8.58. FT-IR (KBr pellets, cm^{-1}): 3036, 2961, 2917, 2873, 2851, 1592, 1513, 1492, 1467, 1376, 1313, 1279, 1177, 883, 813, 752, 695. MS (MALDI-TOF): 2033.0 (M^+). Elemental analysis: Calcd for $\text{C}_{154}\text{H}_{126}\text{N}_4$: C, 91.00; H, 6.25; N, 2.76. Found: C, 90.52; H, 6.56; N, 2.30.

3. Results and discussion

3.1. Synthesis

Oligomer **8** was built from 2,6-dibromoanthraquinone, fluorene boric ester and triphenylamine boric ester, and the synthesis procedure is shown in Scheme 1, and the detailed preparation and characterization of the oligomer are listed in experimental section. **8** was an amorphous powder and can easily form a film on a glass plate by using a spin-coating method, suggesting that the oligomer possesses good solution-processability, which is desire for the fabrication of the optoelectronic devices.

3.2. Thermal stability and optical properties

Thermal properties of **8** were characterized by differential scanning calorimetry (DSC), and the result is shown in Fig. 1. As can be seen from Fig. 1, **8** shows a glass transition temperature, T_g , of 223 °C, which is higher than those of most of the well-known small molecule materials used in optoelectronic fields [18], and even higher than those of some polymeric materials [19], indicating that the oligomer possesses high thin film morphological stability. Moreover, no obvious crystallization peak was observed during a scanning from 50 to 300 °C, demonstrating that **8** has a limited tendency to crystallize.

The basic photophysical properties of **8** were characterized by UV-Vis and photoluminescent (PL) spectra. The

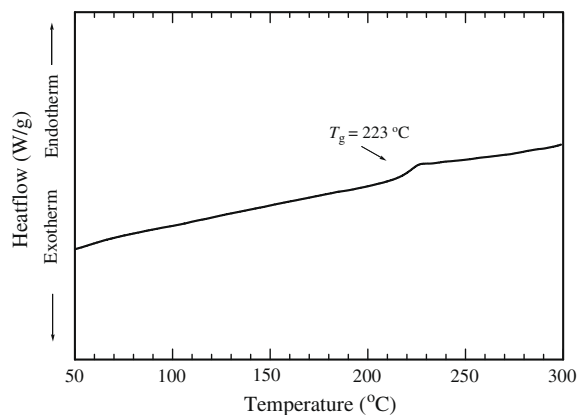


Fig. 1. DSC trace of **8**.

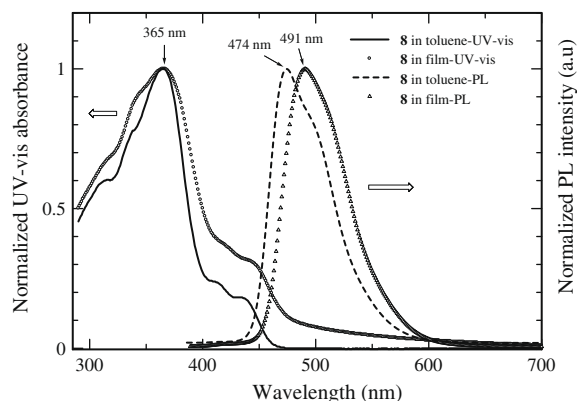


Fig. 2. UV-Vis and PL spectra of **8** in toluene and in the solid state.

spectra are displayed in Fig. 2. The oligomer exhibits a maximum absorption peak at 365 nm in both toluene and in the solid state, whereas the onset position of its absorption band in the solid state has a red-shift, suggesting the existence of part π -stacking structure in the oligomer. It is noted that a compound composed of a fluorene unit and two triphenylamine units showed an absorption peak at about 370 nm [20], thus, the maximum absorption peak at 365 nm in Fig. 2 is attributed to the electronic transition (π - π^*) along the backbone of a fluorene unit linked with a triphenylamine group. The weak absorption peaks at 400–450 nm are also observed in Fig. 2, which are probably derived from the anthracene unit in **8**, the similar absorption peaks were found in our previous work concerning a polymer containing anthracene unit as side chain [21].

The photoluminescent (PL) spectrum of **8** in toluene shows a main peak at 474 nm with a quantum yield of 62% (estimated with a 0.5 M H_2SO_4 solution of quinine as a reference), similar to the PL spectra of poly(9,9-alkylfluorene-alt-triphenylamine) [22]. In the solid state, **8** gives a maximum emission peak at 491 nm with an absolute PL quantum yield of 24%, measured by using a calibrated integrating sphere. Here, the main emission peak of **8** has a red-shift of 17 nm relative to that in the solution, indicating the existence of the interaction between the molecules in the solid state, similar phenomena were also observed in poly(9,9-alkylfluorene-alt-triphenylamine) [23] and the fluorene-anthracene compounds [24].

3.3. Electrochemical properties

The electrochemical behavior of **8** was measured by cyclic voltammetry (CV) of its cast film on a Pt plate, and the result is shown in Fig. 3. The electrochemical oxidation (or p-doping) of **8** starts at about 0.60 V versus Ag^+/Ag , and gives a p-doping peak at 1.02 V. The corresponding reduction peak appears at 0.18 V. According to the relationship between the oxidation onset potential ($E_{\text{ox}}^{\text{onset}}$) and HOMO level value as $-(E_{\text{ox}}^{\text{onset}} + 4.4)$ [24], the HOMO energy level of **8** is estimated as $-(0.60 + 4.4) = -5.00$ eV. Relative to the triphenylamine derivatives with HOMO value of about 5.7 eV, that of **8** is close to the work function of ITO glass (4.5–4.8 eV) [25]. This result implies that **8** is very suitable for OLEDs as a hole-transport layer (HTL). Consequently,

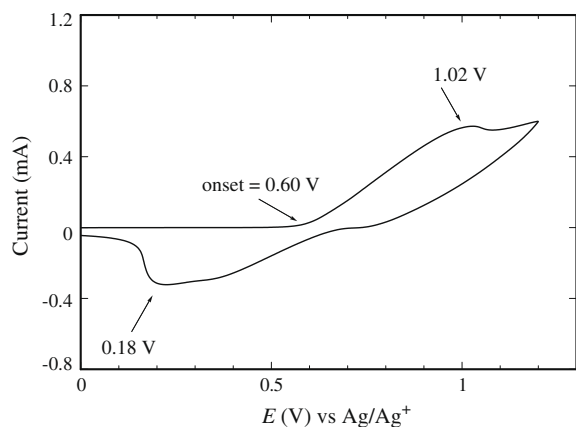


Fig. 3. CV curve of a cast film of **8** on a Pt electrode (wire) with a sweep rate of 100 mV s^{-1} in an acetonitrile solution of $0.10 \text{ M [Bu}_4\text{N]ClO}_4$. The applied potential is $0.0\text{--}1.5 \text{ V}$.

the LUMO value of **8** is calculated by subtraction of the optical bandgap E^{opt} (eV) from the HOMO value, given as -2.41 eV .

3.4. Electroluminescence properties

To evaluate the performance of **8** as a HTL in OLEDs, three non-optimized OLED devices were fabricated with

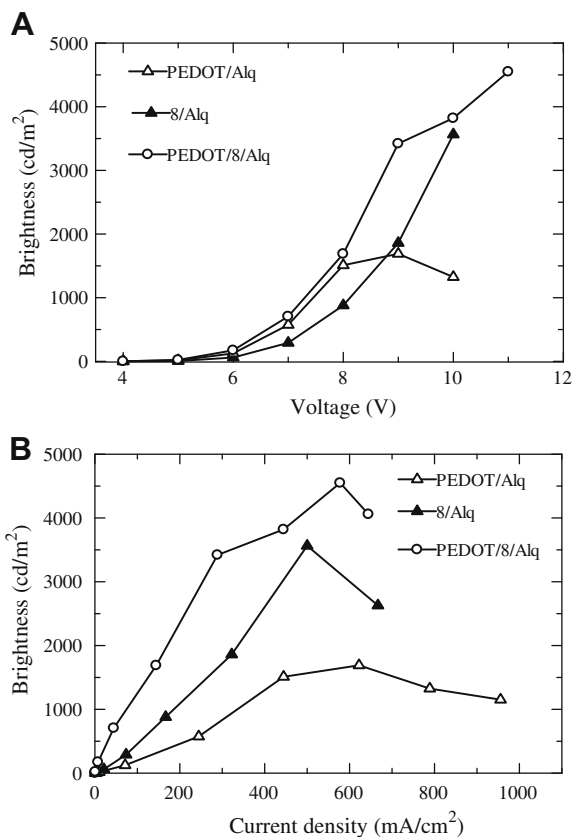


Fig. 4. $B\text{--}V$ (A) and $B\text{--}I$ curves (B) of the three devices.

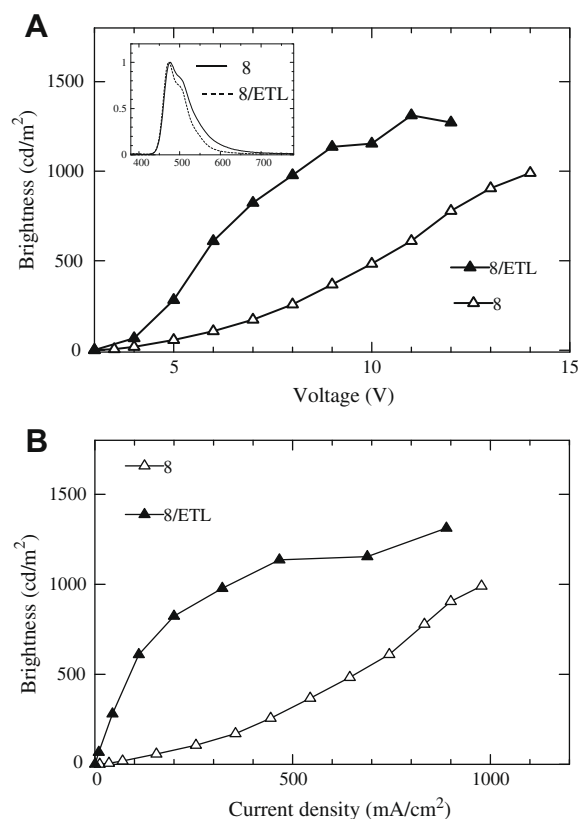


Fig. 5. $B\text{--}V$ (A) and $B\text{--}I$ curves (B) of a device based on **8**.

the following configuration: (1) ITO/PEDOT:PSS/Alq/LiF/Ca/Al (device PEDOT/Alq); (2) ITO/**8**/Alq/LiF/Ca/Al (device **8**/Alq) and (3) ITO/PEDOT:PSS/**8**/Alq/LiF/Ca/Al (device PEDOT/**8**/Alq). Here, PEDOT-PSS was employed as a hole-injection material that had been widely used in OLEDs. Moreover, a commercially available electron transport layer and emitting layer, Alq, was used as both electron transport layer and emitting layer. All devices showed green emission derived from Alq, illuminating that the holes from the anode (ITO) and the electrons from the cathode (Ca/Al) combine in the Alq layer. The $B\text{--}V$ (brightness versus operation voltage) and $B\text{--}I$ (brightness versus current density) characteristics of the devices shows in Fig. 4. As can be seen from Fig. 4, device **8**/Alq shows a maximum brightness of about 3600 cd/m^2 at 10 V , which is much higher than that of the device PEDOT/Alq only with PEDOT as a hole-injection layer, suggesting that oligomer **8** shows good hole-transport ability. Interestingly, when **8** was used together with PEDOT-PSS, the device (PEDOT/**8**/Alq) shows higher brightness and luminous efficiency. Its maximum brightness was 4549 cd/m^2 at 11 V and the maximum current efficiency reached 2.32 cd/A . Moreover, the maximum external quantum efficiencies (Max EQE) of the devices showed an order of PEDOT/Alq (0.11%) < **8**/Alq (0.26%) < PEDOT/**8**/Alq (0.57%). Those results indicate that a combination of **8** and a commercial PEDOT-PSS may obtain a better performance in OLEDs, and that oligomer **8** could be used as a new component in OLEDs.

The high absolute PL quantum yield of **8** inspired us to investigate its application in OLED as a light-emitting layer. A device was fabricated with the configuration of ITO/PED-OT:PSS/**8**/LiF/Ca/Al (device 8). The *B*–*V* curve and efficiency of the device are shown in Fig. 5. As shown in Fig. 5, device 8 shows light-blue emission with a maximum emission peak of 478 nm, which has a slight blue-shift relative to that of its PL emission in the solid state. Device 8 exhibits a low turn-on voltage of 3.5 V, whereas its efficiency is very low (maximum current efficiency = 0.1 cd/A, and Max EQE = 0.043%). This may be due to the unbalance between the hole-transport and the electron transport in the device, derived from the strong hole-transporting ability of **8**. Considering the good electron transport of a bitriazine derivative developed by our group [26], we designed a new configuration of the device using the bitriazine derivative as electron transport layer (ETL) to adjust the balance between the electron transport and the hole-transport in the device. The new device has a configuration of ITO/PED-OT:PSS/**8**/ETL/LiF/Ca/Al (device 8/ETL), and shows the same emission color as that of device 8 with a maximum emission peak of 474 nm (Fig. 5, the insert), but its efficiency is much higher than that of device 8 (for device 8/ETL, maximum current efficiency = 0.6 cd/A and Max EQE = 0.29%), implying that **8** also shows good emitting properties.

4. Conclusion

A new anthracene derivative containing four triphenylamine groups was prepared. Such oligomer is solution-processible with a glass transition temperature of higher than 200 °C, and it showed good hole-transporting ability in organic light-emitting diodes. Such compound was also employed as the emitting layer to give the devices showing blue emission.

Acknowledgements

Financial support from National Natural Science Foundation of China (NSFC, No. 20872171) is gratefully acknowledged. Q. Fang thanks the financial support from Key Laboratory of Advanced Display and System Applications (Shanghai University), Ministry of Education of China (No. A.05-0408-07-003).

References

- [1] (a) W.J. Oldham, R.J. Lachicotte, G.C. Bazan, *J. Am. Chem. Soc.* 120 (1998) 2987; (b) S. Wang, W.J. Oldham, R.A. Hudack, G.C. Bazan, *J. Am. Chem. Soc.* 122 (2000) 5695.
- [2] (a) P.L. McGrier, K.M. Solntsev, J. Schonhaber, S.M. Brombosz, L.M. Tolbert, U.H.F. Bunz, *Chem. Commun.* (2007) 2127; (b) A.J. Zuccherro, J.N. Wilson, U.H.F. Bunz, *J. Am. Chem. Soc.* 128 (2006) 11872; (c) W.W. Gerhardt, A.J. Zuccherro, J.N. Wilson, C.R. South, U.H.F. Bunz, M. Weck, *Chem. Commun.* (2006) 2141.
- [3] J.A. Marsden, J.J. Miller, L.D. Shirtcliff, M.M. Haley, *J. Am. Chem. Soc.* 127 (2005) 2464.
- [4] (a) H. Kang, P. Zhu, Y. Yang, A. Facchetti, T.J. Marks, *J. Am. Chem. Soc.* 126 (2004) 15974; (b) H. Kang, G. Evmenenko, P. Dutta, K. Clays, K. Song, T.J. Marks, *J. Am. Chem. Soc.* 128 (2006) 6194.
- [5] C. Lambert, W. Gaschler, G. Noll, M. Weber, E. Schmalzlin, C. Brauchle, K. Meerholz, *J. Chem. Soc. Perkin Trans. 2* (2001) 964.
- [6] S. Sengupta, P. Purkayastha, *Org. Biomol. Chem.* 1 (2003) 436.
- [7] H.C. Yeh, R.H. Lee, L.H. Chan, T.Y.J. Lin, C.T. Chen, E. Balasubramaniam, T.-Y. Tao, *Chem. Mater.* 13 (2001) 2788.
- [8] S. Fratiloiu, K. Senthilkumar, F.C. Grozema, H. Christian-Pandya, Z.I. Niazimbetova, Y.J. Bhandari, M.E. Galvin, L.D.A. Siebbeles, *Chem. Mater.* 18 (2006) 2118.
- [9] S. Sengupta, S. Muhuri, *Tetrahedron Lett.* 45 (2004) 2895.
- [10] D. Lalibert, T. Maris, J.D. Wuest, *Can. J. Chem.* 82 (2004) 386.
- [11] (a) Z. Xie, B. Yang, F. Li, G. Cheng, L. Liu, G. Yang, H. Xu, L. Ye, M. Hanif, S. Liu, D. Ma, Y. Ma, *J. Am. Chem. Soc.* 127 (2005) 14152–14153; (b) Z. Xie, B. Yang, G. Cheng, L. Liu, F. He, F. Shen, Y. Ma, S. Liu, *Chem. Mater.* 17 (2005) 1287.
- [12] (a) A. Zen, A. Bilge, F. Galbrecht, R. Alle, K. Meerholz, J. Grenzer, D. Neher, U. Scherf, T. Farrell, *J. Am. Chem. Soc.* 128 (2006) 3914; (b) A. Bilge, A. Zen, M. Forster, H. Li, F. Galbrecht, B.S. Nehls, T. Farrell, D. Neher, U. Scherf, *J. Mater. Chem.* 16 (2006) 3177.
- [13] (a) C.W. Wu, H.H. Sung, *J. Polym. Sci. Polym. Chem.* 44 (2006) 6765; (b) J.X. Yang, X.T. Tao, C.X. Yuan, Y.X. Yan, L. Wang, Z. Liu, Y. Ren, M.H. Jiang, *J. Am. Chem. Soc.* 127 (2005) 3278.
- [14] (a) X.B. Sun, Y.Q. Liu, S.Y. Chen, W.F. Qiu, G. Yu, Y.Q. Ma, T. Qi, H.J. Zhang, X.J. Xu, D.B. Zhu, *Adv. Funct. Mater.* 16 (2006) 917; (b) H.Y. Wang, J.C. Feng, G.A. Wen, H.J. Jiang, J.H. Wan, R. Zhu, C.M. Wang, W. Wei, W. Huang, *New J. Chem.* 30 (2006) 667.
- [15] X.M. Liu, J. Xu, X. Lu, C. He, *Macromolecules* 39 (2006) 1397.
- [16] (a) M.T. Bernius, M. Inbasekaran, J. O'Brien, W.S. Wu, *Adv. Mater.* 12 (2000) 1737; (b) U. Scherf, E.J.W. List, *Adv. Mater.* 14 (2002) 477; (c) K. Danel, T.H. Huang, J.T. Lin, Y.T. Tao, C.H. Chuen, *Chem. Mater.* 14 (2002) 3860; (d) A.K. Tripathi, M. Heinrich, T. Chen, J.P. Siegrist, *Adv. Mater.* 19 (2007) 2097; (e) A.C. A Culligan, J.U. Wallace, K.P. Klubek, C.W. Tang, S.H. Chen, *Adv. Funct. Mater.* 16 (2006) 148.
- [17] (a) D.W. Price, J.M. Tour, *Tetrahedron* 59 (2003) 3131; (b) S.K. Lee, W.J. Yang, J.J. Choi, C.H. Kim, S.J. Jeon, B.R. Cho, *Org. Lett.* 7 (2005) 323; (c) Y.J. Pu, T. Kurata, M. Soma, J. Kido, H. Nishide, *Synth. Met.* 143 (2004) 207.
- [18] S.A. Van Slyke, C.H. Chen, C.W. Tang, *Appl. Phys. Lett.* 69 (1996) 2160.
- [19] (a) E. Bellmann, G.E. Jabbour, R.H. Grubbs, N. Peyghambarian, *Chem. Mater.* 12 (2000) 1349; (b) C. Schmitz, P. Pösch, M. Thelakkt, H.W. Schmidt, A. Montali, K. Feldman, P. Smith, C. Weder, *Adv. Funct. Mater.* 11 (2001) 41; (c) X.C. Li, Y.Q. Liu, M.S. Liu, A.K.Y. Jen, *Chem. Mater.* 11 (1999) 1568; (d) J.P. Liu, A.R. Hlil, A.S. Hay, T. Maïndron, J.P. Dodelet, J. Lam, M. D'iorio, *J. Polym. Sci. Polym. Chem.* 38 (2000) 2740.
- [20] Q. Fang, B. Xu, B. Jiang, H. Fu, W. Zhu, X. Jiang, Z. Zhang, *Synth. Met.* 155 (2005) 206.
- [21] J. Du, Q. Fang, D. Bu, S. Ren, A. Cao, X. Chen, *Macromol. Rapid Commun.* 26 (2005) 1651.
- [22] M. Redecker, D. Bradley, M. Inbasekaran, W. Wu, E. Woo, *Adv. Mater.* 11 (1999) 241.
- [23] W. Cui, Y. Wu, H. Tian, Y. Geng, F. Wang, *Chem. Commun.* (2008) 1017.
- [24] S. Janietz, D.D.C. Bradley, M. Grell, C. Giebeler, M. Inbasekaran, E.P. Woo, *Appl. Phys. Lett.* 73 (1998) 2453.
- [25] T. Ishida, H. Kobayashi, Y. Nakato, *J. Appl. Phys.* 73 (1993) 4344.
- [26] H. Zhong, E. Xu, D. Zeng, J. Du, J. Sun, S. Ren, B. Jiang, Q. Fang, *Org. Lett.* 10 (2008) 709.